Open Research Online

The Open University's repository of research publications
and other research outputs

Characterizing Rock Abundance At ExoMars Landing Site Candidates

Conference or Workshop Item

For guidance on citations see FAQs.

Version: Version of Record

Link(s) to article on publisher's website:
http://www.hou.usra.edu/meetings/lpsc2016/pdf/1918.pdf

oro.open.ac.uk

CHARACTERIZING ROCK ABUNDANCE AT EXOMARS LANDING SITE CANDIDATES. E. Sefton-Nash[1,4] (e.sefton-nash@uclmail.net), J. C. Bridges[2], L. Kissick[1], F. Butcher[3], P. Donnelly[2], J. D. Piercy[2], J. L. Vago[4], D. Loizeau[5], L. Lorenzoni[4], P. M. Grindrod[1], M. Balme[3]. [1]Dept. of Earth & Planetary Sciences, Birkbeck, University of London, UK. [2]Space Research Centre, Dept. of Physics & Astronomy, University of Leicester, UK. [3]Dept. of Physical Sciences, The Open University, Milton Keynes, UK. [4]European Space Agency, ESTEC 2200 AG Noordwijk, The Netherlands. [5]Laboratoire de Géologie de Lyon, Université Claude Bernard Lyon 1, France.

Introduction: We present preliminary work to characterize surface rock abundance at ExoMars Rover landing site candidates. A challenge in quantifying the abundance of surface rocks is using the population of large (≥1 m) rocks that are resolved in orbital images to infer the size of the smaller, unresolved rock population. This is particularly relevant for the ExoMars Rover mission, where the Landing Module's clearance of 35 cm [1] makes it necessary to know the probability of encountering rocks where $0.35 < D < 1$ m.

'Float rocks' are individual fragments of rock not associated with a continuous outcrop or body of rock —*e.g.* transported rocks or impact debris. These can be identified in Mars Reconnaissence Orbiter HiRISE [2] images, where the mid-afternoon local solar time, dictated by MROs' orbit, causes float rocks to appear as bright sunlit features adjacent to strong shadows. However, the smallest features resolvable in HiRISE images occupy around 3-4 pixels, corresponding to ~1-m sized rocks. This inherently limits the ability to directly identify from orbit the small, but potentially hazardous rock population. 'Outcrop' is defined as continuous expanses of bedrock or surficial deposits exposed at the surface [3]. Both float rocks and outcrop can contribute to slopes that may constitute a hazard for landed missions.

We present rock counts at ExoMars Rover landing site candidates and assess approaches to constrain the morphological characteristics of Mars' surface that are relevant to rover and lander safety.

Rock abundance model: Rock abundance (RA) is often quantified as the areal fraction, F, of a surface covered by rocks with diameter ≥D. The canonical rock distribution model [4] was established by fitting an exponential curve to the cumulative rock size frequency distribution (SFD) at the Viking landing sites. The small rock population, where $D < 1$ m, was found to fit well to the relationship $F_k(D) = ke^{-q(k)D}$, where $q(k) = 1.79 + 0.152/k$, and k is the 'rock abundance factor'. By fitting a rock SFD to the model, a single value of k can be retrieved for a rock population.

The model was derived using rocks observed in image mosaics of the near- and far-field in the immediate vicinity of the Viking landers. The small rock population was well resolved, but due to the small total area observable from the landers, few large rocks were present in the SFDs. The model is therefore a useful

tool for estimating the abundance of otherwise unresolvable small rocks based on the SFD of large rocks, though suffers from a lack of in-situ validation for large rock diameters. Typically, the model is used in conjunction with thermally-derived RA, orbital imagery, geological inferrences and available in-situ results to infer rock populations [5, 6].

Method: We have conducted preliminary manual counting of float rocks at candidate landing sites using HiRISE [2] observations. We selected 68 sub-frames 500x500 m² in size from map-projected HiRISE images. Locations were selected to adequately sample the diversity of geologic units, and to maximize spatial coverage within landing ellipses.
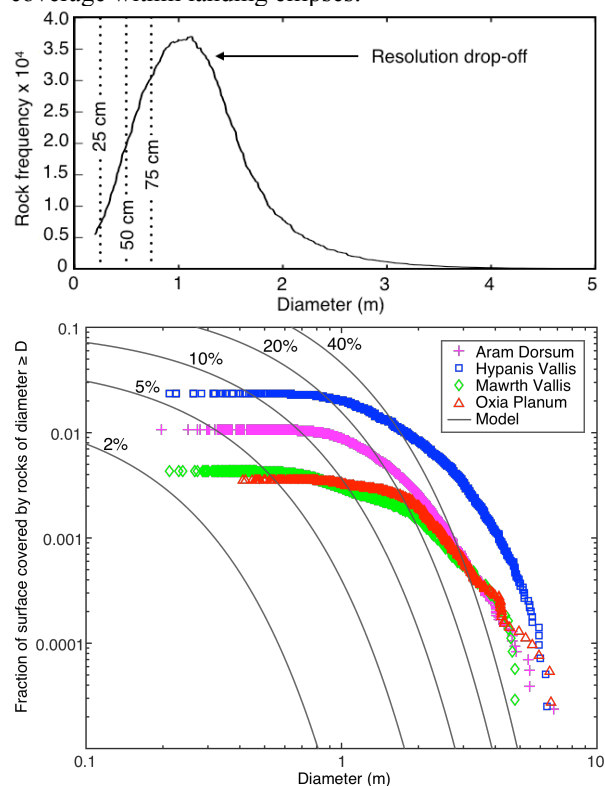

Figure 1. Upper: Size frequency distribution of 46893 features identified as rocks in sampled areas of HiRISE images at the 4 sites assessed. Lower: Cumulative fractional area curves for each site. Model values of $F_k(D)$ calculated using equs. 11 and 12 in [4] are plotted for 2, 5, 10, 20 and 40% total fractional areas.

In several count areas, repeat counts were performed to test the consistency of rock identification between human counters. A total of 46893 features were identified in 68 unique counts, plus 6 repeats, covering 17 km² over 4 landing site candidates.

Results/Discussion: We observe that the drop-off in feature identification caused by the HiRISE resolution limit begins when D≈1.2 m (Fig. 1), equivalent to ~4–5 map-projected HiRISE pixels. Many features are identified at sizes below this, but the drop in frequency with decreasing diameter is contrary to the SFD shape expected at small diameters. We also observe that consistency between human counters was generally good, but that discrepancies occurred most frequently in areas of shadow-casting outcrop, where it was difficult to distinguish isolated float rocks from rocky outcrop. Large scale local slopes, such as wrinkle ridges, cause a change in the local solar illumination angle and therefore shadow length. This caused differences in human ability to identify features on sun-facing slopes compared to on those facing away from solar incidence. Nonetheless, we propose that representative RAs may be obtained manually with sufficiently large count areas, such that sources of uncertainty are averaged across broad areas. For quantification of the total hazard due to short length-scale slopes, both float rocks and rough outcrop features should be mapped.

Thermally-derived rock abundance: Thermal inertia (TI) of the Martian surface has been derived using various datasets [e.g. 7, 8] and may be used as a proxy for RA [9]. Anisothermality, the effect of observing different apparent radiances in thermal IR for the same field of view, but in different bandpasses, is attributed to contrasting temperatures caused by materials with different thermal properties. Generalization of the surface's thermal reponse as a 2-component signal originating from high and low thermal inertia materials allows retrieval of the apparent RA, and the low thermal inertia 'fine component' [9].

This technique has been applied to data from thermal IR datasets to retrieve RA. However, uncertainties in such techniques stem from assumptions made about the rock size distribution that contributes to the thermal signal. For example, an uncertainty of ±20% was estimated for the Viking IRTM RA due to the assumption that all rocks contributing to the thermal signal had a fixed thermal inertia, corresponding to an effective diameter of ~0.15 m [9].

Values of thermally-derived RA correspond to much higher cumulative fractional areas than we observe in our rock counts. This disparity is due to two major effects: 1) The small rock population that is unresolved from orbit contributes to the thermal signal, and 2) Flat, high TI materials, e.g. outcropping rock surface, also contribute to the thermal signal [10, 11], but do not cast shadows, so are not identified as rocks.

Conclusions: The exponential fit [4] provides a good estimate of RA at the Viking landing sites, which include mainly float rocks transported by large channel outflows, but few outcrops. It remains to be demonstrated, however, that the same family of curves and parameters should result in equally good fits when applied to sites whose geology has been sculpted by other processes—such as the ExoMars candidate sites. It is likely that, for locations including both float rocks and a large outcrop fraction, the laws governing the statistical properties of rock distribution and outcrop roughness may be quite different. The size and distribution of float rocks depends on how they were created and scattered (*i.e.* impacts, water transport), but the texture of outcrops is mainly determined by their nature (*i.e.* volcanic, sedimentary, etc.) and erosional strength. For example, soft outcrop units may be flat and relatively devoid of debris; conversely, hard units may retain rough edges and constitute obstacles for landing/locomotion. Large variations in RA may therefore be expected within any landing site, linked to the presence of different geological units, and rock-rich features such as ejecta from recent impact craters.

It is clear that to constrain the probability of encountering slopes that may be hazardous to surface craft, an approach is required that integrates visible/IR remotely-sensed data as well as in-situ rock counts from landed missions. Manual identification of features in orbital images requires sufficient coverage and repeat counts to quantify uncertainty, but remains a principle technique in assessing the probability of encountering hazardous features. Small rocks (D <1m) that are unresolved from orbit, as well as flat and high TI terrains, contribute to thermally-derived RA. However, effective use of thermal RA to quantify the small rock population requires constraint of thermal contributions from different features and terrain types.

The use of high resolution thermal data [8], super-resolution imaging techniques [12] and detailed geological inferences may be key techniques in ongoing assessment of ExoMars Rover landing site candidates.

References: [1] ExoMars 2018 Landing Site Selection User's Manual (2013), ESA (EXM-SCI-LSS-ESA/IKI-003). [2] McEwen, A. S. et al. (2007), *J. Geophys. Res.* 112 (E05S02). [3] Lorenzoni, L. V. et al. (2013), EXM-MS-RS-ESA-00013 (Iss.5, Rev.1), ESA. [4] Golombek, M. and Rapp, D. (1997), *J. Geophys. Res.* 102 (E2) p. 4117–4129. [5] Golombek, M. P. et al. (2008), *J. Geophys. Res.* 113, E00A09. [6] Golombek, M. P. et al. (1997), *J. Geophys. Res.* 102 (E2), p. 3967–3988. [7] Nowicki, S. A. and Christensen, P. R. (2007), *J. Geophys. Res.* 112(E05007). [8] Audouard, J. et al. (2014), *Icarus* 233, p. 194–213. [9] Christensen, P. R. (1986), *Icarus* 68, p. 217–238. [10] Binder A. B. et al. (1977), *J. Geophys. Res.* 82 (28) p. 4439 – 4451. [11] Moore, H. J. and Keller, J. M. (1990), *Reports of Plan. Geology & Geophys. Program*, NASA Tech Memo. TM 4210, p. 533–535. [12] Tao, Y. and Muller, J.-P. (2015), *Plan. & Space Sci.*, In Press.